Journal of Structural Geology, Vol. 6, No. 5, pp. 571 to 578, 1984
Printed in Great Britain

0191-8141/84 $03.00 + 0.00

The calculation of a best-fit ellipsoid from elliptical sections on arbitrarily orientated planes

W. H. OWENS

Department of Geological Sciences, University of Birmingham, P.O. Box 363, Birmingham, B15 2TT, U.K.

(*Received* 17 *August* 1982; *accepted in revised form* 22 *November* 1983)

Abstract—A two-stage procedure is described for the calculation of a best-fit ellipsoid from elliptical sections measured on three or more arbitrary planes. The first stage produces an initial, trial solution. This is used as a starting point for a standard, linear, least-squares treatment to determine the best-fit ellipsoid.

Factors influencing the reliability of a solution (for example, number of measurements and quality of data) are discussed in the context of real and synthetic examples. The examples indicate that the procedure described is relatively robust and they allow guidelines for its routine practical application to be suggested.

INTRODUCTION

WHERE measurements of elliptical sections on three or more arbitrarily orientated planes are available, they may be combined to define an ellipsoid. The problem is essentially one of scaling the ellipse sections to represent a common ellipsoid; where redundant data indicate a degree of mismatch between the sections, the scaling must distribute the error appropriately. The elliptical sections may be measured directly, as, for example, where reduction spots are used for strain estimation, or they may be generated by one of the many methods of two-dimensional strain analysis, which can make use of a variety of strain markers.

Solutions relating to the problem of ellipsoid estimation have been presented by a number of authors. At the simplest level, for the case where sections on principal planes are available, the three-axis plot provides a rapid method of arriving at a visually best-fitting solution (Owens 1974). For the more general case of an arbitrarily orientated set of three orthogonal planes, Helm & Siddans (1971) employed a matrix formalism to calculate the suite of six ellipsoids which arise by matching all possible combinations of elements in the matrices describing the section ellipses; these ellipsoids can then be averaged visually. This method has been decribed more fully by Shimamoto & Ikeda (1976). Mathematical approaches, tackling the problem of a matching directly and attempting to produce single 'optimum' solutions, have been described by Oertel (1978), for the case of data on three orthogonal planes, and by Milton (1980) and Gendzwill & Stauffer (1981), for the case of data on three arbitrary planes.

In this paper a two-stage technique for the calculation of a best-fitting ellipsoid from data on three or more section planes is described. In the first stage a somewhat arbitrary scaling procedure is used to provide a set of initial solutions; one of these is then used, in the second stage, as a starting value for a procedure of least-squares refinement which leads, iteratively, to a best-fitting solution. In comparison with previous papers on the three-dimensional problem of ellipsoid estimation, more emphasis has been placed on attempts to test the method, by using it to analyse sets of synthetic data (for which the true solutions are obviously known). The synthetic data can incorporate random perturbations, due to a variety of causes, so that the response of the method to noisy data can be evaluated and criteria developed for assessing the reliability of a solution. No attempt has been made to consider systematic effects, which may bias the data.

THEORY

Although the theory refers to the general mathematical problem of solving for a best-fit ellipsoid, the most obvious application in structural geology is to the determination of the strain ellipsoid and it is convenient to cast the argument in these terms. Thus given a strain **S** which relates a line before strain, denoted by the vector $\mathbf{r}_i$, to the corresponding line after strain, denoted by $\mathbf{r}_f$

$$\mathbf{r}_f = \mathbf{S}\mathbf{r}_i. \tag{1}$$

Consider its effect on a sphere of unit radius, defined by

$$\mathbf{r}_i^T\mathbf{r}_i = 1 \tag{2}$$

where $\mathbf{r}_i^T$ is the transpose of $\mathbf{r}_i$. Substituting (1) in (2) the equation of the strain ellipsoid is

$$\mathbf{r}_f^T(\mathbf{S}^{-1})^T(\mathbf{S}^{-1})\,\mathbf{r}_f = 1. \tag{3}$$

If the strain is written as a product of pure shear and rotation

$$\mathbf{S} = \mathbf{P}\mathbf{R} \tag{4}$$

(3) becomes

$$\mathbf{r}_f^T(\mathbf{P}^{-1})^T(\mathbf{P}^{-1})\mathbf{r}_f = 1$$

or

$$\mathbf{r}_f^T\mathbf{P}^{-1}\mathbf{P}^{-1}\mathbf{r}_f = 1 \tag{5}$$

which is the mathematical expression of the fact that the

strain ellipsoid carried no information about any rotational component of strain (e.g. Owens 1973).

In the general case **P** is a symmetric, second rank tensor, but if it is diagonalized and so referred to its principal axes

$$\mathbf{P} = \begin{bmatrix} a & & \\ & b & \\ & & c \end{bmatrix} \tag{6}$$

and (5) becomes the familiar

$$x^2/a^2 + y^2/b^2 + z^2/c^2 = 1. \tag{7}$$

By introducing

$$\mathbf{Q} = \mathbf{P}^{-1}\mathbf{P}^{-1} \tag{8}$$

equation (5) can be written

$$\mathbf{r}_f^{\mathrm{T}}\mathbf{Q}\mathbf{r}_f = 1. \tag{9}$$

Q is a symmetric, second rank matrix. Its principal axes are those of **P** and its principal values are related to those of **P** as

$$q_i = 1/p_i^2. \tag{10}$$

The q_i are reciprocal quadratic elongations (Ramsay 1967, p. 66).

The initial problem is to determine the elements of **Q** in eqn (9). At this stage, concern is primarily with ellipsoid shape rather than absolute size, so one element can be assigned arbitrarily and five remain to be determined. To find these from ellipses measured on planes intersecting the ellipsoid, an equation is required for the elliptical trace seen on such a plane (Ramberg 1976). Rather than solve the problem of a general plane intersecting the ellipsoid, it is more convenient to view the problem with respect to a set of axes (x_e, y_e, z_e) within and perpendicular to the plane, the axes within the plane being taken parallel to the principal axes of the ellipse. Referred to these axes, an ellipse of axial ratio r_e has equation

$$x_e^2/r_e^2 + y_e^2 = 1/C, \tag{11}$$

where C is a scaling factor. (The ellipse axes are $r_e/C^{1/2}$, $1/C^{1/2}$). This equation may be written as

$$[x_e \quad y_e]\begin{bmatrix} C/r_e^2 & \\ & C \end{bmatrix}\begin{bmatrix} x_e \\ y_e \end{bmatrix} = 1. \tag{12}$$

If **A** is the rotation matrix relating the reference axes (x, y, z) and the (x_e, y_e, z_e) axis set, such that

$$\mathbf{r}_e = \mathbf{A}\mathbf{r}, \tag{13}$$

then (9) becomes

$$\mathbf{r}_e^{\mathrm{T}}\mathbf{A}\mathbf{Q}\mathbf{A}^{\mathrm{T}}\mathbf{r}_e = 1 \tag{14}$$

or, if

$$\mathbf{W} = \mathbf{A}\mathbf{Q}\mathbf{A}^{\mathrm{T}}, \tag{15}$$

$$[x_e \quad y_e \quad z_e]\begin{bmatrix} w_{11} & w_{12} & w_{13} \\ w_{21} & w_{22} & w_{23} \\ w_{31} & w_{32} & w_{33} \end{bmatrix}\begin{bmatrix} x_e \\ y_e \\ z_e \end{bmatrix} = 1 \tag{16}$$

and the intersection with the xy plane (defined by $z = 0$) can simply be written, in matrix terms, as

$$[x_e \quad y_e]\begin{bmatrix} w_{11} & w_{12} \\ w_{21} & w_{22} \end{bmatrix}\begin{bmatrix} x_e \\ y_e \end{bmatrix} = 1. \tag{17}$$

(The intersection with a parallel plane, say at $z = d$, simply alters the constant on the right hand side.)

The formal identity of equations (17) and (12) gives rise to three equations:

$$\begin{aligned} w_{11} &= C/r_e^2 \\ w_{12} &= w_{21} = 0 \\ w_{22} &= C. \end{aligned} \tag{18}$$

The elements of **W** combine the unknown elements of **Q** with the known elements of the rotation matrix **A**. Thus, from a single plane we have three equations for six unknowns: the five elements of **Q** and the scaling factor. Specifically, if $q_{33} = 1$ is set arbitrarily

$$\begin{aligned} &a_{11}^2q_{11} + 2a_{11}a_{12}q_{12} + 2a_{11}a_{13}q_{13} \\ &\qquad + a_{12}^2q_{22} + 2a_{12}a_{13}q_{23} - C/r_e^2 = -a_{13}^2 \\ &a_{11}a_{21}q_{11} + (a_{11}a_{22} + a_{12}a_{21})q_{12} + (a_{11}a_{23} + a_{13}a_{21})q_{13} \\ &\qquad + a_{12}a_{22}q_{22} + (a_{12}a_{23} + a_{13}a_{22})q_{23} = -a_{13}a_{23} \\ &a_{21}^2q_{11} + 2a_{21}a_{22}q_{12} + 2a_{21}a_{23}q_{13} + a_{22}^2q_{22} \\ &\qquad + 2a_{22}a_{23}q_{23} - C = -a_{23}^2. \end{aligned} \tag{19}$$

These may be rewritten in matrix form as

$$\begin{bmatrix} a_{11}^2 & 2a_{11}a_{12} & 2a_{11}a_{13} & a_{12}^2 & 2a_{12}a_{13} \\ a_{11}a_{21} & a_{11}a_{22} & a_{11}a_{23} & a_{12}a_{22} & a_{12}a_{23} \\ & +a_{12}a_{21} & +a_{13}a_{21} & & +a_{13}a_{22} \\ a_{21}^2 & 2a_{21}a_{22} & 2a_{21}a_{23} & a_{22}^2 & 2a_{22}a_{23} \end{bmatrix}$$

$$\begin{bmatrix} -1/r_e^2 & \\ 0 & \\ -1 & \end{bmatrix}\begin{bmatrix} q_{11} \\ q_{12} \\ q_{13} \\ q_{22} \\ q_{23} \\ C \end{bmatrix} = \begin{bmatrix} -a_{13}^2 \\ -a_{13}a_{23} \\ -a_{23}^2 \end{bmatrix}. \tag{20}$$

Symbolically this may be written, using partitioned matrices, as

$$[\mathbf{A}_1' \quad \mathbf{r}_1]\begin{bmatrix} \mathbf{q} \\ C_1 \end{bmatrix} = [\mathbf{a}_1'] \tag{21}$$

where the subscript signifies the first plane. Expanding this to take account of more intersecting planes, for example three planes

$$\begin{bmatrix} \mathbf{A}_1' & \mathbf{r}_1' & 0 & 0 \\ \mathbf{A}_2' & 0 & \mathbf{r}_2' & 0 \\ \mathbf{A}_3' & 0 & 0 & \mathbf{r}_3' \end{bmatrix}\begin{bmatrix} \mathbf{q} \\ C_1 \\ C_2 \\ C_3 \end{bmatrix} = \begin{bmatrix} \mathbf{a}_1' \\ \mathbf{a}_2' \\ \mathbf{a}_3' \end{bmatrix} \tag{22}$$

where the matrices are of order 9×8, 8×1 and 9×1, respectively. In the general case, for n planes, the dimensions are $(3n, n + 5)$, $(n + 5, 1)$, and $(3n, 1)$. For $n \geq 3$ there are more independent equations than unknowns and a solution for the overdetermined equations can be

obtained. Golub's method for a least-squares solution, as described by Claerbout (1976, p. 116 and fig. 6-1) has been used.

It is important to note that the solution obtained at this stage is not a 'best-fit' solution, since the equations are not cast in the appropriate form. In the standard, linear least-squares problem

$$\mathbf{Mx} = \mathbf{b} \tag{23}$$

is solved, where **b** is a column vector of observations, **x** is the column vector holding the solution and **M** is the matrix relating the observations and solution. The optimum, least-squares solution is that which minimizes the sum of squares of differences between the observed values of **b** and those predicted from the solution

$$\begin{aligned} \delta\mathbf{b} &= \mathbf{b} - \mathbf{Mx} \\ \delta\mathbf{b}^{\mathrm{T}}\delta\mathbf{b} &= \text{minimum.} \end{aligned} \tag{24}$$

In eqn 22, however, the observed quantities, which are the orientations and axial ratios of the elliptical sections, are scattered through both the matrix on the left hand side and the vector on the right. No obvious physical significance can be attached to the quantity that is minimized. It is, indeed, possible to recast the equations, not on the basis of $q_{33} = 1$ as in (19), but by applying this normalizing condition to the five other elements, q_{ij}; all six solutions are routinely sought. For perfect input data each of these six sets of equations yields the correct solution. For imperfect data the solutions diverge, and if the data are sufficiently noisy, some (or occasionally all) of the solutions may lead to negative eigenvalues and thus give results which cannot be interpreted as ellipsoids.

If a solution to an equation like (22) can be obtained, its value is that it can provide a starting point, which may be close enough to the final solution to allow a linear treatment to be adopted in a process of least-squares refinement (e.g. Clifford 1973). In this process the discrepancies between the observed quantities and those calculated from the initial solution are used to derive a series of adjustments to the starting values. Clearly the adjusted values can be treated in a similar fashion, so the procedure can be carried out iteratively.

In the present case a set of observations consists of the strike and dip of a plane, the pitch of an ellipse long axis within this plane and the axial ratio of the ellipse. It is assumed that the strike and dip can be measured with negligible error; thus the case is only considered where, for a variety of reasons (e.g. non-sphericity of the original markers), the observations of pitch and axial ratio r_e may be in error.

The direct use of the observed values of pitch and axial ratio as the vector of observations, **b** in equation (23), raises problems. In setting up a least-squares solution it is implicit (if arbitrary weighting is not to be introduced) that all the error terms (i.e. the elements of $\delta\mathbf{b}$ in 24) are of the same order. Since the error in pitch is related to the axial ratio of the ellipse (the major axis becomes indeterminate as the ellipse becomes circular), this condition is not satisfied and a more appropriate choice for the vector **b** must be sought.

If it is argued that scatter arises principally from non-sphericity in the original markers, some guidance may be drawn from the equation given by Ramsay (1967, eqn. 5.24, p. 208), connecting the fluctuation, or maximum deviation of ellipse major axis direction from the extensional strain direction (ϕ_{max} in Ramsay's notation) with the initial ellipse axial ratio, r_e, and the strain ellipse ratio, r_t. A tongue-in-cheek development of the equation proceeds as follows: for small axial ratios r_e write

$$r_e - 1 = \delta r_e.$$

Then, from a development of Ramsay's equation, to first order in r_e,

$$\tan 2\phi_{max} = 2r_t\delta r_e/(r_t^2 - 1)$$

so that, for small ϕ_{max} (which implies r_e small compared with r_t)

$$(r_t - 1/r_t)\phi_{max} \approx \delta r_e$$

But

$$\ln r_e = \ln (1 + \delta r_e) = \delta r_e \ldots$$

therefore

$$(r_t - 1/r_t)\phi_{max} \approx \ln r_e. \tag{25}$$

The consequences of this approximation may be compared with the results plotted by Ramsay (1967, fig. 5.26, p. 208). The development is roughly equivalent to approximating the familiar pear-shaped contour on an Rf/ϕ plot (Dunnett 1969) by an ellipse of axial ratio $(r_t - 1/r_t)$. It implies that fluctuation values, when multiplied by $(r_t - 1/r_t)$, are of the same order as $\ln r_e$. It must be emphasized that the treatment is approximate only, but it leads to the suggestion that appropriate variables to use in the minimization procedure of (24) are

$$b_{2i} = \ln r_i$$

and

$$b_{2i+1} = (r_t - 1/r_t)\chi_i \tag{26}$$

so that

$$\delta b_{2i} = \ln r_i - \ln r_{ti} = \ln r_i/r_{ti} = \ln r_{ei}$$

and

$$\delta b_{2i+1} = (r_t - 1/r_t)(\chi_i - \chi_{ti}), \tag{27}$$

where r_i and χ_i are the observed axial ratio and pitch of the ellipse on the ith section and r_{ti} and χ_{ti} are the values calculated for that section from the trial ellipsoid, so that the last two equations relate, respectively, to the initial ellipse axial ratio and to the fluctuation.

In a linear least-squares refinement solution, the error vector $\delta\mathbf{b}$ is related to the adjustment $\delta\mathbf{q}$ in the ellipsoid parameters by

$$\Sigma \frac{\partial b_i}{\partial q_j}\,\delta q_i = \delta b_i, \tag{28}$$

where the summation is taken over five of the six values of q, since the set of initial values has been scaled so that one value, say q_{33}, has unit magnitude.

For three or more planes, equations of the form of eqn (28) can be expressed in the standard matrix form for least-squares refinement:

$$\begin{bmatrix} \text{Matrix of} \\ \text{differentials} \end{bmatrix} \begin{bmatrix} \text{Column} \\ \text{vector} \\ \delta\mathbf{q} \end{bmatrix} = \begin{bmatrix} \text{Column} \\ \text{vector} \\ \delta\mathbf{b} \end{bmatrix} \quad (29)$$

with dimensions, for n planes, of $(2n, 5)$ 5 and $2n$, respectively. These may be solved for the adjustments $\delta\mathbf{q}$ by Golub's method, referred to above. In the present treatment the matrix of differentials has not been derived analytically, but has been approximated by calculating the differences Δb which arise from two values of q separated by a small difference Δq about the value for the trial solution. The elements of the vector $\mathbf{q}$, adjusted by the values of $\delta\mathbf{q}$, are used to construct the matrix $\mathbf{Q}$ (equation 8) which can then be diagonalized to give the directions and magnitudes of the reciprocal quadratic elongations, and hence of the principal axes of the ellipsoid.

APPLICATION AND EVALUATION

In this section results will be discussed which have been obtained using programs based on the analysis described above. The calculation proceeds in two stages: first a series of initial, trial solutions is sought; any one of these can then be taken and refined, in the second stage, to obtain the best-fit ellipsoid. No formal treatment of errors of estimation for the best-fit ellipsoid has been derived. However the program, in addition to calculating an ellipsoid, also produces measures and summary parameters which can be used to gauge the reliability of a solution. The examples below have been chosen to illustrate the influence of different factors on the quality of a solution and the role of the error indices in assessing that quality.

The first example, of reduction spot measurements on a single block, illustrates the nature of the primary data required for the programs and the form of results, both solution. In the first of these are considered the results of examples investigate the significance of the error measures and their relationship to the reliability of the solution. In the first of these are considered the result of a series of simulation exercises on synthetic data in which the effects of sample size, initial particle shape and reading error are examined. Finally, on the basis of the last example, the discussion is extended to examine the response of the programs to gross errors (arising, for example, from misreading). This example again uses reduction-spot data, which were in this case collected in the field.

Block sample, N. Wales

In Table 1 are listed measurements of reduction spots made on an unorientated block of slate from Dinorwic, N. Wales. Where repeated measurements, say N, have been made on a given plane or on nearly parallel planes, they have been weighted as $1/N^{1/2}$. Table 2 gives the five (out of six) trial solutions which produced ellipsoids and the final, best-fit solution to which all the trial solutions converged; in the table natural strains are normalized to $\Sigma\epsilon_i = 0$ and thus refer to an ellipsoid of volume 4π. The input data are plotted on a stereogram in Fig. 1(a). Principal axis directions for the trial and best-fit solutions are shown in Fig. 1(b) and the strain magnitudes are presented on a three-axis planar diagram (Owens 1974)

Table 1. Input data

Strike	Dip	Pitch	Long axis (mm)	Short axis (mm)	Axial ratio	Weight
−58	78	165	16.5	4.5	3.67	0.58
−59	77	166	9.5	3.5	2.71	0.58
122	105	14	20.5	6.8	3.01	0.58
21	109	7	37.0	6.0	6.17	1.00
−2	109	0	7.5	1.5	5.00	1.00
198	101	170	16.7	3.0	5.57	0.58
197	102	172	22.0	4.0	5.50	0.58
199	102	173	18.0	3.0	6.00	0.58

Table 2. Trial and best-fit solutions

	Maximum axis			Intermediate axis			Minimum axis		
Basis	Natural strain	Declination	Dip	Natural strain	Declination	Dip	Natural strain	Declination	Dip
$q_{33} = 1$	0.91	32	10	0.14	305	−13	−1.05	86	−73
$q_{11} = 1$	1.39	227	−12	−0.13	319	−9	−1.26	85	−74
$q_{13} = 1$	1.29	40	12	−0.07	313	−10	−1.23	82	−74
$q_{22} = 1$	0.82	17	6	0.17	289	−16	−0.98	86	−73
$q_{23} = 1$	0.89	31	10	0.16	304	−14	−1.05	86	−73
Best-fit	0.85	29	10	0.18	302	−14	−1.03	85	−73

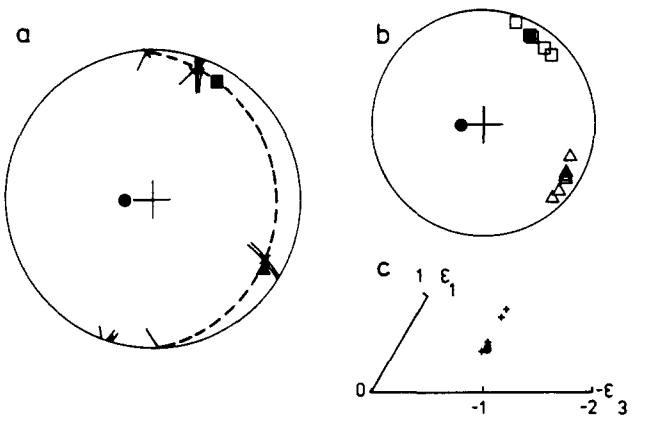

Fig. 1. Reduction spot measurements from an unorientated block, Dinorwic, N. Wales. (a) Data planes are indicated by partial traces about the pitch of reduction spot long axes, marked by crosses. The principal axis directions for the best-fit ellipsoid are plotted as solid symbols (maximum, square; intermediate, triangle; minimum, circle). The dashed line is the trace of the plane containing the maximum and intermediate ellipsoid axes. (b) Stereogram of principal axis directions for the trial (open symbols) and best-fit (closed symbols) ellipsoids. Axis convention as in (a). (c) Three-axis plot for the trial (crosses) and best-fit (solid circle) ellipsoids.

in Fig. 1(c). (Where, as in this figure and in Fig. 4, the plot conveys information on ellipsoid shape alone, only the sector defined by the major and minor axes ϵ_1 and ϵ_3, is plotted.)

For comparison with the input data, the program calculates the values of ellipse axial ratio and pitch predicted for the observed planes from the ellipsoid solution. For each plane the calculated section ellipse can be used to 'unstrain' the observed ellipse to produce a notional 'undeformed ellipse'. These results are given in Table 3. The weighted log-mean of the undeformed ellipse axial ratios, denoted by ρ, can be used as a measure of goodness of fit. For this example the value of ρ is 1.10; the significance of this value will be discussed in the light of the experiments with synthetic data.

Simulation exercises

The input data for these experiments were derived from a program which applies a specified strain to randomly orientated ellipsoids of given axial ratio and calculates the resulting ellipse sections on randomly orientated planes. Systematic effects, arising from the fact that the trial solutions are tied to the reference axis frame (by setting specific elements q_{ij} to 1; see eqn 19), are avoided by orientating the principal strain axes randomly with respect to the reference axes.

Table 3. Section data calculated for planes of observation

Strike	Dip	Pitch	Axial ratio	Undeformed ellipse axial ratio
−58	78	165	3.15	1.17
−59	77	165	3.14	1.16
122	105	15	3.08	1.06
21	109	7	6.26	1.03
−2	109	1	4.88	1.07
198	101	172	5.70	1.26
197	102	173	5.61	1.06
197	102	172	5.72	1.11

The results of the simulations are given in Figs. 2 and 3. The calculated principal axis directions are plotted sterographically in the principal axis frame of the applied strain and magnitudes are given on three-axis plots (Owens 1974). Where a set of results is closely coaxial, the full three-axis plot may be used to convey both magnitude and relative directional information (e.g. interchange of minimum and intermediate axes; see Fig. 2f). Where the principal axes are scattered, the results, plotted in one sector only, carry information about magnitude alone, and must be interpreted in conjunction with the stereograms of principal axis directions. An intermediate case, which arises in the simulations given below, is that in which one axis only is closely related to the principal axis frame of the applied strain; here some measure of directional information has been preserved in the three-axis plots by indicating, with a dashed line bounded by the calculated values, a range of solutions between sectors.

In the examples two initial ellipsoid shapes have been considered. The examples using axial ratios of 1.1:1.0:0.91 relate to cases either where strain markers can be taken as originally nearly spherical, or where the ellipse sections for given planes have been derived by some method of two-dimensional strain analysis to this order of precision. Examples using axial ratios of 1.3:1.0:0.67 are more relevant to analyses (e.g. of deformed conglomerates) in which there is a pronounced initial ellipsoid shape. In all the cases considered, a strain of 1.65:1.0:0.25 (natural strains $\epsilon_x = 0.80$, $\epsilon_y = 0.30$, $\epsilon_z = -1.09$), representative of values found in slate belts (Wood 1974), has been applied.

Two aspects of the method of analysis are considered: firstly, the interaction of initial ellipsoid shape and sample size in determining the accuracy of the solutions and, secondly, the manner in which the method reacts to random errors in variables not considered in developing the analysis.

(i) *Initial ellipsoid shape and sample size.* Three sample sizes, of 3, 10 and 30 sections have been adopted; for the case of three sections, both randomly orientated and orthogonal sets are examined. In all cases ten different sets of data have been generated; for some of these no solution could be obtained.

The results are given in Figs. 2(a–d & f–i). They demonstrate that, as expected, accuracy increases with increasing sample size and with decreasing initial ellipsoid axial ratio. In the case of samples of three sections, however, it is salutary to note how much better are solutions based on orthogonal, rather than random, sections.

The log-means of the undeformed ellipse axial ratios, ρ, are plotted in Fig. 3. From a comparison of the scatter

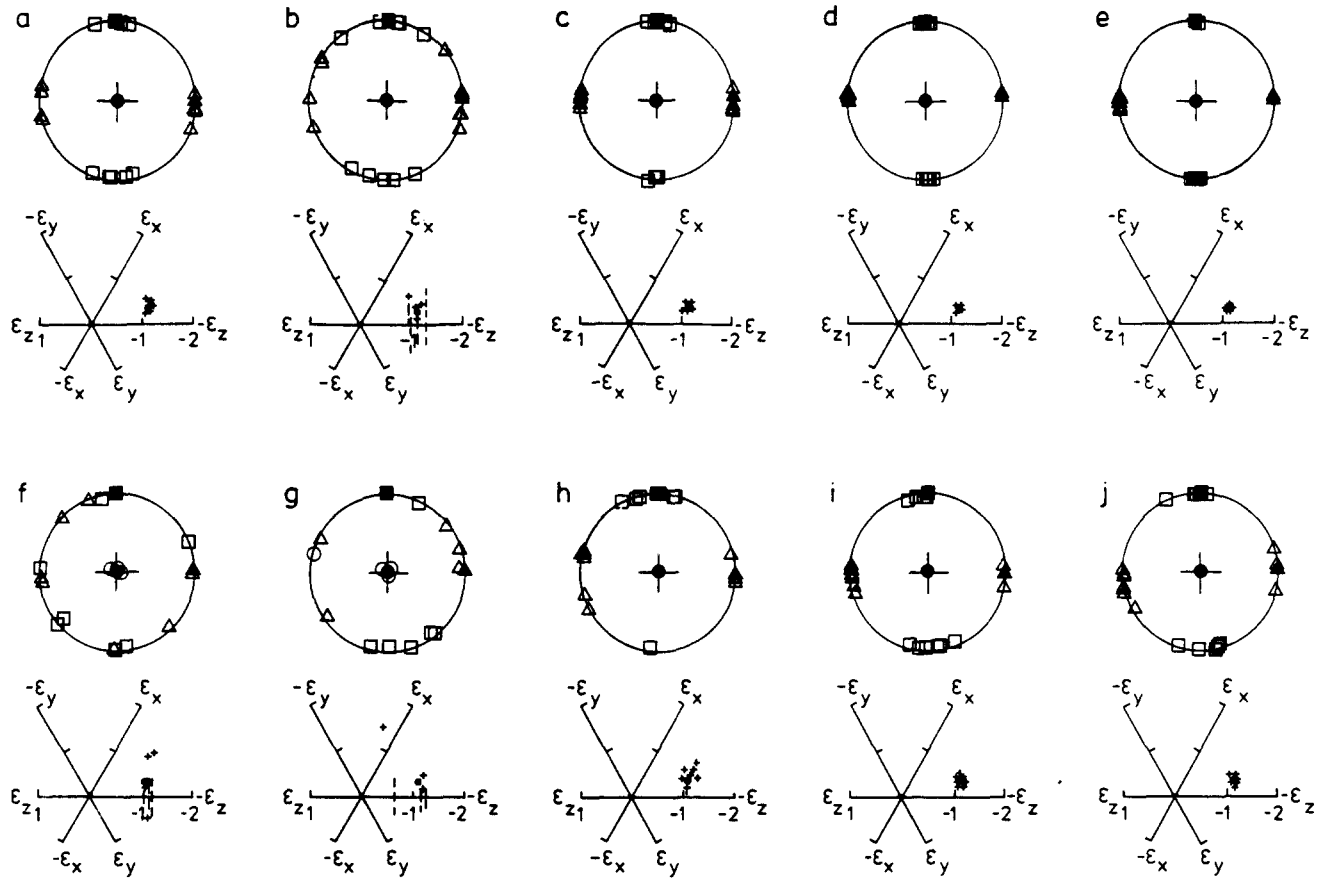

Fig. 2. Synthetic data generated for a strain of $\epsilon_x = 0.80$, $\epsilon_y = 0.30$ and $\epsilon_z = -1.09$, for varying combinations of initial ellipsoid axial ratio and number of data planes. Stereograms and three-axis plots for successful best-fit solutions from, in each case, ten randomly generated data sets. In the stereograms, the x axis is vertical, z into the paper. Upper row: initial ellipsoid 1.1:1.0:0.91. Lower row: initial ellipsoid 1.3:1.0:0.67. (a) & (f): 3 orthogonal sections; (b) & (g): 3 random sections; (c) & (h) 10 random sections; (d) & (i): 30 random sections and (e) & (j): 30 random sections, angular data perturbed by random error of 3° standard deviation.

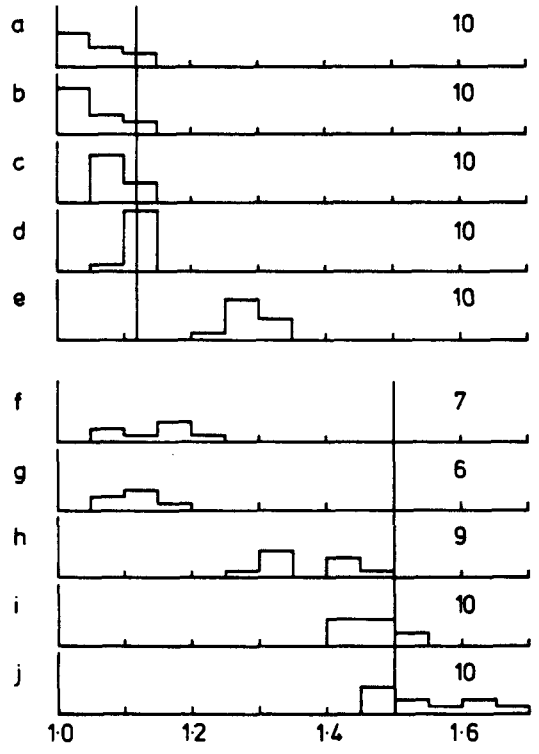

Fig. 3. Histograms of log-mean undeformed ellipse axial ratios, ρ, for the solutions, from synthetic data, given in Fig. 2. The number of successful solutions (out of ten) is shown at the right. The log-mean ellipse axial ratio, ρ_i, for 1.1:1.0:0.91 and 1.3:1.0:0.67 ellipsoids are respectively, 1.12 and 1.50.

of solutions shown in Fig. 2 with the values of ρ in Fig. 3, it is clear that ρ cannot, on its own, be used as a positive indication of the accuracy of a solution. Closeness of the value of ρ to unity merely indicates how well the sections on which the solution is based combine to form an ellipsoid; the probability of such fortuitous conjunctions obviously decreases with increasing sample size. Associated with a particular initial ellipsoid shape there is a particular value of ρ, say, ρ_i; for the two ellipsoid shapes adopted in these simulations the values are respectively 1.12 and 1.50. If, in practice, the initial value ρ_i were known, the calculated values of ρ could be used, negatively, to reject solutions, were there a large difference, of either sign, between ρ and ρ_i. A small difference would not, however, necessarily imply that the solution was reliable.

It is appropriate, at this point, to reconsider the example given in Fig. 1. Although the solution shows a high degree of internal consistency ($\rho = 1.10$), it should be noted that it is, effectively, based on only four planes which are not evenly spaced. Further measurements would clearly be desirable.

(ii) *Random reading errors*. The method of analysis assumes that errors arise only in ellipse axial ratio and pitch, so that the orientation of the plane of section is known accurately. The effect of reading errors in section

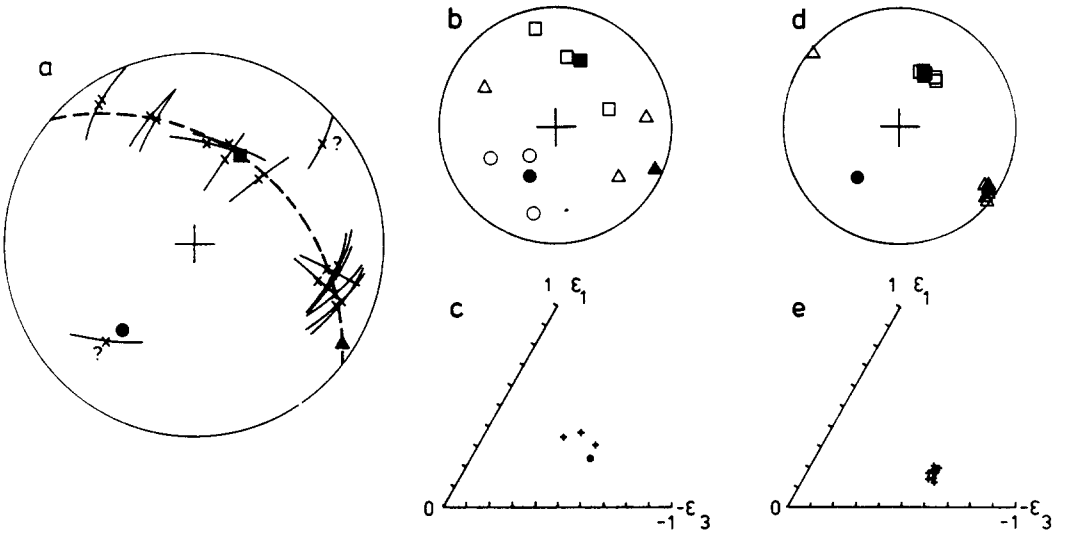

Fig. 4. Reduction spot measurements from Val de Blore, Alpes Maritimes; conventions as in Fig. 1. (a) Input data and best-fit ellipsoid solution from (d, e) below. (b, c) Trial and best-fit solutions based on all data, equally weighted. (d, e) Trial and best-fit solutions omitting data queried in (a).

plane orientation must therefore be examined. Further, at high strains, fluctuation (in the sense of Ramsay 1969, p. 202) is small so that reading error may be a significant source of variation. These effects have been investigated by perturbing the angular data in the previous sets by a normally distributed error of specified standard deviation. (This rather simple model neglects the interrelationship of errors in strike and dip; see Woodcock 1976). The results for samples of 30 sections, with a reading error of 3° standard deviation, are given in Figs. 2(e & j). The effect of the perturbation is, as might be expected, to increase the scatter of solutions and to increase the value of the log-mean undeformed ellipse axial ratio.

Field data, Alpes Maritimes

When presented with a data set containing erroneous readings the programs will, in most cases, produce a solution, so it is important to develop criteria for recognizing the presence of bad data. The effect of gross errors in the data is illustrated in Fig. 4. The data are of reduction spots in the Permian red-beds of the Alpes Maritimes, measured at exposures near Val de Blore. For a flattening strain one expects that the long axes of the measured ellipses will, in general, lie in or close to the plane of flattening. In Fig. 4 two long axes diverge considerably from the swath defined by the rest of the data. The solution including these two data has $\rho = 1.44$; that ignoring them has $\rho = 1.15$. The ellipses in question have axial ratios and long axis pitches of 1.90, 137° and 2.36, 15°, compared with predicted values based on the ellipsoid solution calculated without them, of 2.45, 40° and 2.80, 49°. The observed and calculated axial ratios are in reasonable agreement, so it is possible that the data are truly in error, the first recording pitch from the wrong strike azimuth (137° + 40° ≈ 180°), the second arising as 50° misheard as 15°.

In general the presence of bad data may be indicated in a variety of additional ways.

(a) The value of ρ, the log-mean undeformed ellipse axial ratio, will be greater than one would reasonably expect.

(b) If the rogue data do not overwhelm the solution (they form, say, 10% of readings), they will have, as in the case discussed above, individual 'undeformed ellipse' axial ratios that are markedly high.

(c) If the data set is sufficiently poor to force a compromise solution, the individual predicted ellipse axial ratios will all underestimate the observed values (instead of scattering above and below them).

(d) For consistent, in contrast to poor, data sets, initial trial solutions based on different q_{ij} values will be close and will converge rapidly to a best-fit solution.

CONCLUSIONS

The method described here has been tested against synthetic data and has been applied to a number of field problems (Kligfield *et al.* 1981a, b). Against this background the following guidelines for assessing the reliability of a solution may be established.

(1) Although the minimum number of sections required for a solution is three, and the solution is then marginally overdetermined, it is clearly advantageous to have a greater number of section planes if possible. The number of sections required for a given accuracy of solution will depend on how closely the section data correspond to section ellipses (i.e. sections through the strain ellipsoid) rather than defining ellipses influenced by initial object shape. (Where measurements derive from objects which were not originally spherical, it has been assumed that the orientation of the objects was initially random, otherwise systematic errors would arise.)

(2) Where three sections only are used, they should, if possible, be taken on orthogonal or near-orthogonal planes. In general one should aim for a uniform (rather than random) distribution of planes. The observed planes and ellipse long-axis directions should be plotted on stereograms in the field. This will aid the collection of a uniform spread of data and should eliminate some classes of gross error.

(3) Comparison of observed section ellipses with those predicted from the solution provides an indication of the internal consistency of a solution. The predicted ellipses can be used to 'unstrain' the observed ellipses to provide 'undeformed ellipses'. These should not be influenced strongly by the axial ratios of the ellipsoid and they therefore offer a basis for comparison between solutions. The log-mean undeformed ellipse axial ratio, ρ, has been used as a summary parameter. Low values of ρ indicate a high degree of internal consistency but do not necessarily indicate a solution close to the true strain ellipsoid. The initial shape of the strain markers will, ideally, determine an expected value for ρ. Values below this may arise from a fortuitous conjunction of ellipse sections; the likelihood of this occurring is greater where a small number of sections is involved. Random reading errors in field observations cause the expected value of ρ to rise above the theoretical value for a given shape of marker. So, too, do local departures from uniform strain. Values of ρ much larger than expected suggest that the data set is unreliable; in some cases questionable data items in the set can be identified.

Acknowledgements—For help in the development of the method of analysis, from trial to best-fit solutions, I am indebted to Martin Casey, who has been working on general problems of three-dimensional strain analysis and related error estimation. Roy Kligfield's continued interest and enthusiasm has been a valuable stimulus. Inken Blunk made many perceptive and detailed comments on the manuscript, as also, in their turn, did the reviewers.

REFERENCES

Claerbout, J. F. 1976. *Fundamentals of Geophysical Data Processing.* McGraw-Hill, New York.

Clifford, A. A. 1973. *Multivariate Error Analysis.* Applied Science Publishers, London.

Dunnet, D. 1969. A technique of finite strain analysis using elliptical particles. *Tectonophysics* **7**, 117–136.

Gendzwill, D. J. & Stauffer, M. R. 1981. Analysis of triaxial ellipsoids: their shapes, plane sections and plane projections. *Math. Geol.* **13**, 135–152.

Helm, D. G. & Siddans, A. W. B. 1971. Deformation of a slaty, lapillar tuff in the English Lake District: discussion. *Bull. geol. Soc. Am.* **82**, 523–531.

Kligfield, R., Carmignani, L. & Owens, W. H. 1981a. Strain analysis of a Northern Apennine shear zone using deformed marble breccias. *J. Struct. Geol.* **3**, 421–436.

Kligfield, R., Owens, W. H. & Lowrie, W. 1981b. Magnetic susceptibility anisotropy, strain and progressive deformation in Permain sediments from the Maritime Alps (France). *Earth Planet. Sci. Lett.* **55**, 181–189.

Milton, N. J. 1980. Determination of the strain ellipsoid from measurements on any three sections. *Tectonophysics* **64**, T19–T27.

Oertel, G. 1978. Strain determination from the measurement of pebble shapes. *Tectonophysics* **50**, T1–T7.

Owens, W. H. 1973. Strain modification of angular density distributions. *Tectonophysics* **16**, 249–261.

Owens, W. H. 1974. Representation of finite strain by three-axis planar diagrams. *Bull. geol. Soc. Am.* **85**, 307–310.

Ramberg, H. 1976. The strain in a sheet intersecting the strain ellipsoid at any angle. *Bull. Soc. géol. Fr.* **18**, 1417–1422.

Ramsay, J. G. 1967. *Folding and Fracturing of Rocks.* McGraw-Hill, New York.

Shimamoto, T. & Ikeda, Y. 1976. A simple algebraic method for strain estimation from deformed ellipsoid objects—I. Basic theory. *Tectonophysics* **36**, 315–337.

Wood, D. S. 1974. Current views of the development of slaty cleavage. *A. Rev. Earth Planet. Sci.* **2**, 369–401.

Woodcock, N. H. 1976. The accuracy of structural field measurements. *J. Geol.* **84**, 350–355.